



## Design and Analysis of Wound Field Three-Phase Flux Switching Machine with Non-overlap Windings and Salient Rotor

Faisal Khan, Erwan Sulaiman, Md Zarafi Ahmad, and Zhafir Aizat Husin

Department of Electrical Power Engineering  
Faculty of Electrical and Electronic Engineering, University Tun Hussein Onn Malaysia

*Abstract:* Topologies for three-phase salient rotor flux-switching machines having non-overlap armature and field windings are presented. Salient rotor is used to modulate and switch the polarity of the flux linkage in the armature winding and this phenomenon represents the basic principle of operation of these types of machines. Non-overlap windings and toothed-rotor are the clear advantages of these topologies as the copper losses gets reduce and rotor becomes more robust. Finite Element Analysis (FEA) is used to examine the three phase topology of proposed Wound-field flux switching motor (WFFSM) with non-overlap windings and salient rotor. Coil test analysis, peak armature flux linkage, cogging torque, induced emf and average torque are examined. On the basis of these analyses, it is confirmed that 24S-10P has high flux linkage, less cogging torque and high average torque as compared to other WFFSMs.

*Keywords:* Wound-field flux switching motor (WFFSM), topology, salient rotor, non-overlap windings

### 1. Introduction

In the mid 1950s, the first concept of flux switching machine (FSM) has been founded and printed. 4 stator slots and 4 rotor poles (4S-4P) permanent magnet FSM i.e. permanent magnet single-phase limited angle actuator or more well-known as Laws relay has been developed [1], and then single phase generator with 4 stator slots, and 4 or 6 rotor poles (4S-4/6P) has been invented[2].

Over the last decade, many FSM topologies have been introduced for various application i.e. automotive, domestic appliances, aerospace etc. FSM can be classified into three groups that are permanent magnet (PM) FSM, Field Excitation (FE) FSM and Hybrid Excitation (HE) FSM. PM and field winding are the main sources of flux in PMFSM and FEFSM while in HEFSM, both field winding and permanent magnet produces the flux [3-6]. In all these FSMs, the armature winding and field winding or PM are located on the stator. When compare with other FSMs, the FEFSM motor has advantages of low cost, simple construction, magnet-less machine, and variable flux control capabilities suitable for various performances. Furthermore, to manufacture the FEFSM motors, the PM on the stator of conventional PMFSMs is replaced by DC field excitation coil. In other words, the FEFSM motors having salient-rotor structure is a novel topology, merging the principles of the SRMs and inductor generator [7-8].

The performance of FSM is enhanced by using segmental rotor configuration in recent research [9]. Segmental rotor is designed in a manner such that to achieve bipolar flux in armature winding, which has neither magnets nor winding. To produce bipolar flux linkages in this way, a toothed-rotor structure may be used but it requires overlap windings on the stator [10]. Non-overlap windings have been used in [11] to increase the efficiency by reducing the copper losses and enhanced the speed torque characteristics of FSM. A three-phase FSM using a segmental rotor has been proposed in [12] to improve fault tolerance to a reduction in torque pulsations and power converter rating per phase. Figure 1 [10] and 2 [12] shows FSMs having segmented-rotor with non-overlap windings and toothed-rotor with overlap windings at the stator. A single-phase WFFSM machine was comprehensively investigated in [13-15]. In that

---

Received: August 7<sup>th</sup>, 2014 Accepted: June 8<sup>th</sup>, 2015

machine, armature and field windings are fully pitched and hence the end-winding length is increased. Two single phase WFFSMs topologies with DC field and AC armature windings having the same coil-pitch of 2 slot-pitches and having different coil-pitches of 1 and 3 slot-pitches respectively are discussed [16]. It is shown that the iron loss and copper loss of WFFSM has been reduced and thus increased the efficiency.

This paper explains the feasible topologies, flux linkage, cogging torque, induced emf, average torque and torque speed characteristics for three-phase proposed WFFSM with non-overlap windings and toothed-rotor structure.

## 2. Topologies for three phase WFFSM

The fundamental principle of the flux switching mechanism is that the salient rotor is used to modulate and switch the polarity of the flux linkage in the armature winding. All excitation sources are on the stator with the armature and field allocated to alternate stator teeth. The polarity of each field tooth to change on the alternate field tooth is the requirement for its implementation.

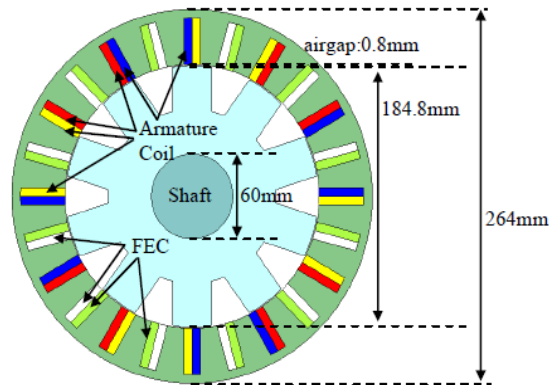


Figure 1. WFFSM with toothed-rotor

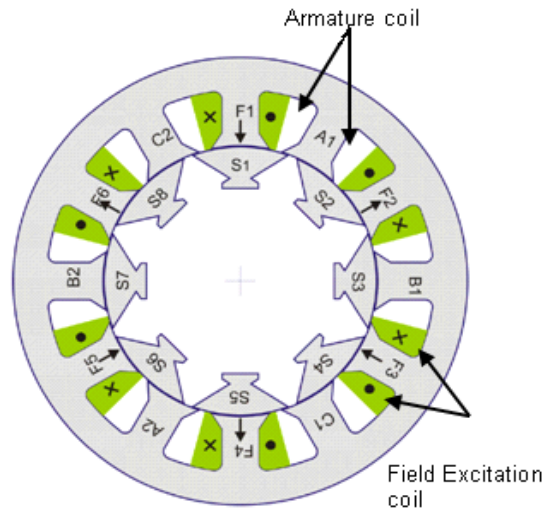


Figure 2. WFFSM with segmented-rotor

For three-phase WFFSM, 6 cannot be the minimum number of stator teeth because if 3 slots are located for armature teeth, the other 3 slots cannot form alternate pairs for field

excitation coil. Thus, under this limitation, the minimum number of stator teeth for three phase WFFSM are 12, 24, 36 etc. The primary investigation therefore considers a 24 teeth stator in which armature winding are placed in 12 slots with phase each comprising four coils, leaving 12 slots for field winding. The use of the field and armature teeth on a 24-tooth stator for the implementation of flux switching principle by means of a toothed-rotor is shown in Figure 3.

Five topologies of 24S-10P, 24S-14P, 24S-16P, 24S-20P, and 24S-22P are evaluated in this investigation as shown in Figure. 4 and the initial design specifications are illustrated in Table 1. All the topologies have non-overlap windings and robust rotor structure.

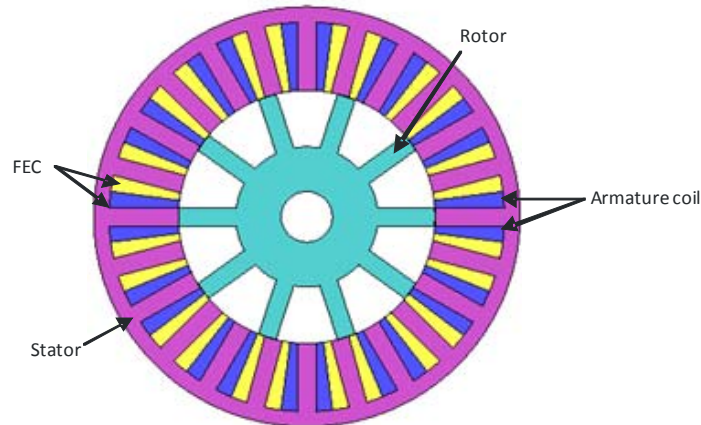


Figure 3. 24Slots-10Poles WFFSM with non-overlap winding and salient rotor

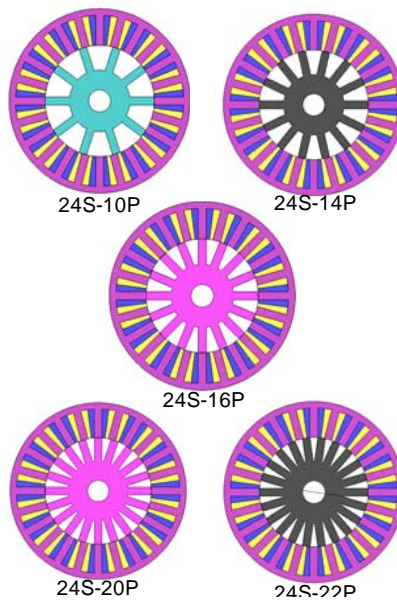


Figure 4. Various topologies of WFFSM

Table 1. WFFSM Design Specification

Outside diameter of stator	300 mm
Width of stator tooth and rotor tooth	13 mm
Back iron depth of stator	11 mm
Motor stack length	80 mm
Length of air gap	0.3 mm
Diameter of rotor	180 mm
Number of turns per FE Coil slot	44
Number of turns per armature coil slot	44
Maximum armature current density, $J_a$	30 Arms/mm <sup>2</sup>
Maximum field current density, $J_e$	30 A/mm <sup>2</sup>
Total armature slot area, $S_a$	414.14 mm <sup>2</sup>
Total field slot area, $S_f$	414.14 mm <sup>2</sup>
Filling factor	0.5

### 3. Design Methodology

The designs are examined using FEA simulations, conducted via JMAG-Designer ver. 13 released by Japan Research Institute (JRI) and the characteristics of each topology are discussed, based on the flux linkages, EMF production, flux distribution and cogging torque. Firstly, JMAG Editor is used to draw the rotor, stator, armature coil and DC Field excitation coil. Then, the materials, conditions, circuits and properties of the machine are set in JMAG Designer. The electromagnetic steel, 35H210 is used for the rotor and the stator core. Moreover, coil arrangement tests are examined to validate the operating principle of WFFSM and to set the position of each armature coil phase.

There are several concepts in designing the three phase configuration using salient rotor. This paper focuses on two main parameters, non-overlap windings and different number of salient rotor poles to design low cost, high efficiency and robust rotor configuration motor.

### 4. FEA Based Performance Analysis

#### A. Coil arrangement test

In order to set the position of each armature coil phase and to confirm the operation principle of WFFSM, coil arrangement test are performed for each armature coil separately, where the FEC are wound in alternate direction and armature coil are wound in anti-clockwise direction as shown in Figure. 5. DC current of 141.185 A is applied to field winding and the flux linkage at each coil is observed. By comparing the flux linkages of different coils, the armature coil phases are defined according to conventional three phase system. Figure 6 illustrates the three-phase flux linkage defined as U, V, and W, respectively. The same procedure is employed for other topologies. The operating principle of WFFSM to get 3-phase flux linkage of the machine has been effectively achieved. Flux linkage waveform of 24S-14P WFFSM has small distortion due to odd harmonics 5, 7 etc. From figure7, it is obvious that 24S-10P has high flux linkage as compare to other WFFSM topologies. This means that the 24S-10P configuration has possibility to provide higher torque and power. For the rest of rotor pole numbers, less amplitude of flux linkage is due to some flux leakage occurs when higher rotor pole number used in the design and will further investigate in the future.

#### B. Induced voltage at open circuit condition

At open circuit condition, the induced voltage generated from FEC with the speed of 1200 r/min for different rotor pole numbers are illustrated in Figure.8. WFFSM with 24S-10P configuration has highest amplitude of approximately 138 V while 24S-14P configuration has less amplitude of 17 V approximately and the waveform is distorted due to odd harmonics 5, 7 etc. Back emf at no load condition of all topologies is less than applied voltage which makes it

easy to provide protection when the inverter is in off state due to some faults.

*C. Cogging Torque Analysis*

The cogging torque analyses for different rotor pole numbers are shown in Figure. 9. WFFSM with 24S-20P configuration has highest peak to peak cogging torque followed by 24S-16P with 64 Nm and 38.0 Nm, respectively while WFFSM with 24S-22P has least peak to peak cogging torque approximately 2Nm. As high cogging torque causes vibration in machine and makes it noisy therefore, further design refinement and optimization will be conducted in future to reduce the cogging torque to an acceptable condition.

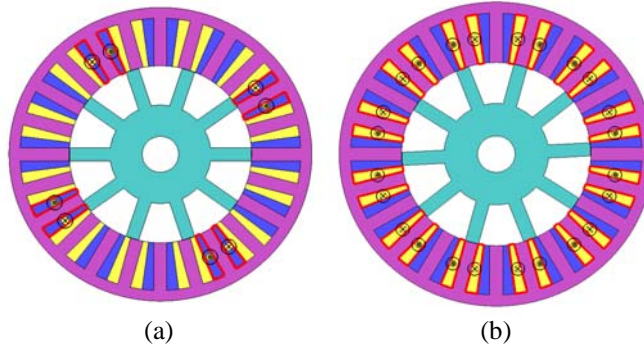


Figure 5. WFFSM coil arrangement test (a) armature coil in anti-clockwise direction (b) FEC in alternate direction

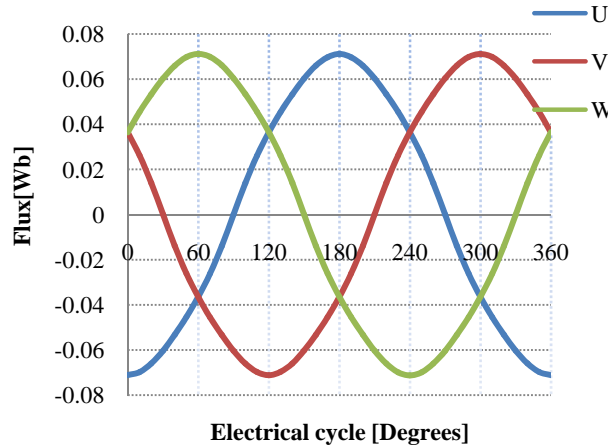


Figure 6. Flux linkages of 24S-10P in terms of U, V, W

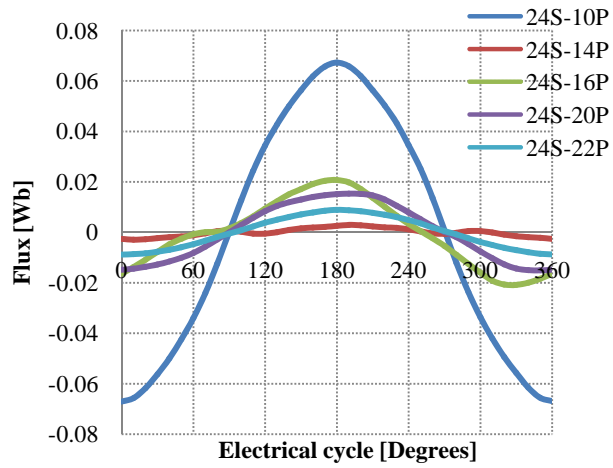


Figure 7. Flux linkage of U-phase

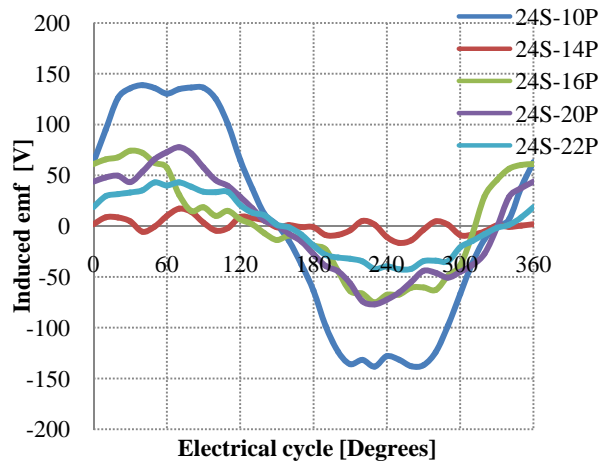


Figure 8. Induced voltages at 1200 rpm

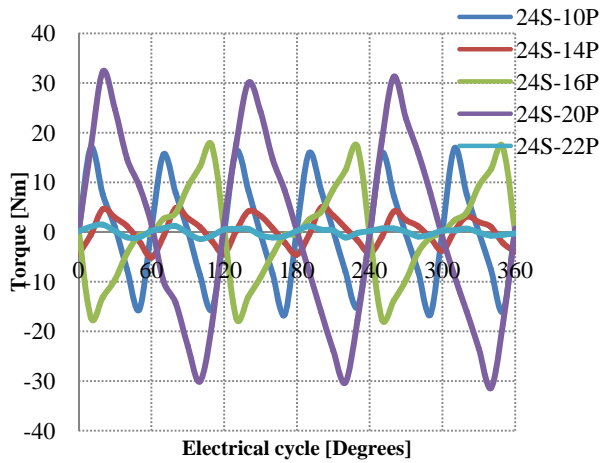


Figure 9. Cogging Torque

*D. Flux Characteristics at Various DC FEC Current Densities,  $J_e$  and Flux Distribution*

Two WFFSM topologies 24S-22P and 24S-10P are chosen to examine their flux characteristics due to less cogging torque and high flux linkage. The flux characteristics for 24S-22P and 24S-10P at various DC FEC current densities,  $J_e$  are illustrated in Figure. 10. It is obvious from both Figures that flux pattern increase linearly by increasing field current density,  $J_e$  until value of 10 A/mm<sup>2</sup>. Then the flux of 24S-22P starts to reduce when high field current density is injected while flux pattern of 24S-10P has increasing value till 30A/mm<sup>2</sup>. It is anticipated that this phenomena happens due to flux cancellation and flux leakage that will be investigated in future. Additionally, 24S-22P WFFSM has 12 more poles than 24S-10P, thus it provide much larger area and more flux distributed. The flux generated by 24S-22P has much less value when compared with 24S-10P WFFSM, as can be seen from Figure. 10. The flux distribution of 24S-22P and 24S-10P WFFSMs at  $J_e$  of 30 A/mm<sup>2</sup> and  $J_a$  of 30 A<sub>rms</sub>/mm<sup>2</sup> are illustrated in Figure.11. More regions of 24S-22P gets saturated when compared with 24S-10P as shown in red circle and the saturation effect can also be confirmed from Figure. 10 that flux line of 24S-22P becomes constant by increasing value of  $J_e$  beyond 15 A/mm<sup>2</sup>. In Figure. 10, there is maximum point for 24S-10P WFFSM at  $J_e$  of 30A/mm<sup>2</sup> and 24S-22P WFFSM at  $J_e$  of 10A/mm<sup>2</sup> which shows the maximum value of flux. From both Figures, it is confirmed that 24S-10P WFFSM has the tendency to generate more flux and less saturation effect.

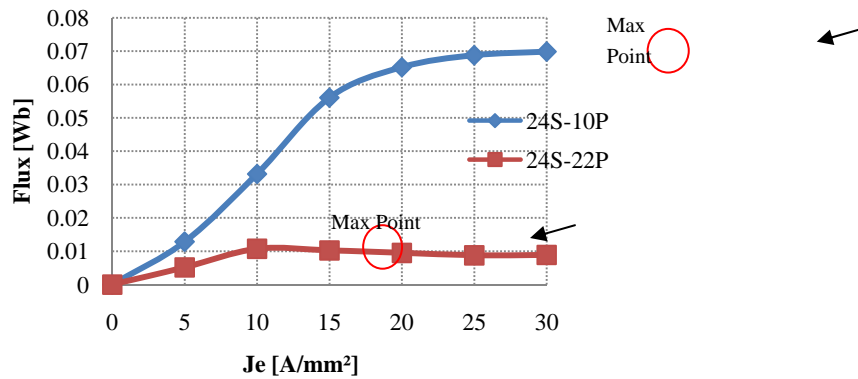


Figure 10. Comparisons of maximum flux vs.  $J_e$  for 24S-10P and 24S-22P WFFSM

*E. Torque Vs. Armature Current Density and Field Current Density Curves*

The torque vs. armature current density,  $J_a$  curves for various field current density  $J_e$  is shown in Figure12 and Figure13. The torque achieved for 24S-10P is approximately 72 Nm at maximum  $J_a$  and  $J_e$  of 30 A/mm<sup>2</sup>, 4.67 times greater than 24S-22P which is 15.42 Nm. At low armature coil current density of 5A<sub>rms</sub>/mm<sup>2</sup>, both machines have same characteristics such that

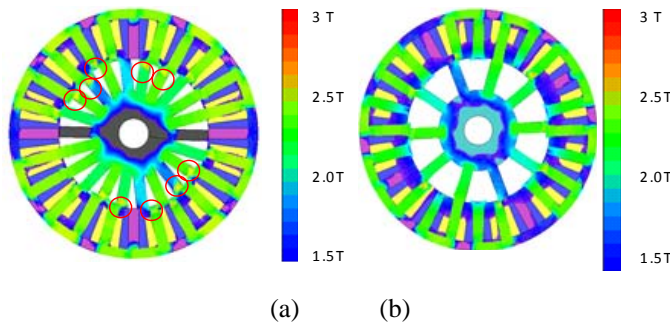


Figure 11. Flux Distribution of WFFSMs (a) 24S-22P (b) 24S-10P

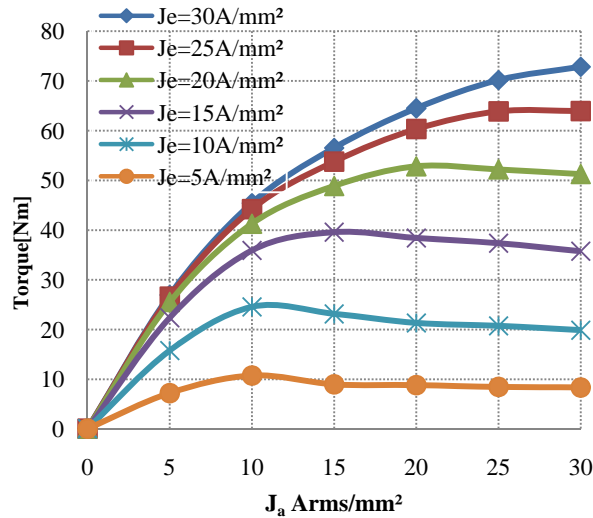


Figure 12. Torque Vs.  $J_a$  at various  $J_e$  for 24S-10P

torque is increased linearly by increasing field excitation coil current density. Then, the torque of 24S-10P WFFSM increases as the load increases and finally reaches a constant value even if the armature coil current density  $J_a$  further increases while the torque of 24S-22P first increases and then decreases by increasing the load. From the comparison of both Figures, it is obvious that 24S-10P design has high torque values.

The instantaneous torque characteristics at maximum field excitation coil and armature coil current densities of  $30\text{A/mm}^2$  and  $30\text{A}_{\text{rms}}/\text{mm}^2$  for both 24S-10P and 24S-22P WFFSMs are depicted in Figure. 14. The peak-to-peak torques generated are approximately 10 Nm and 35 Nm for both machines. Although 24S-10P has high torque ripples but it can be minimized by following the technique discussed in [17].

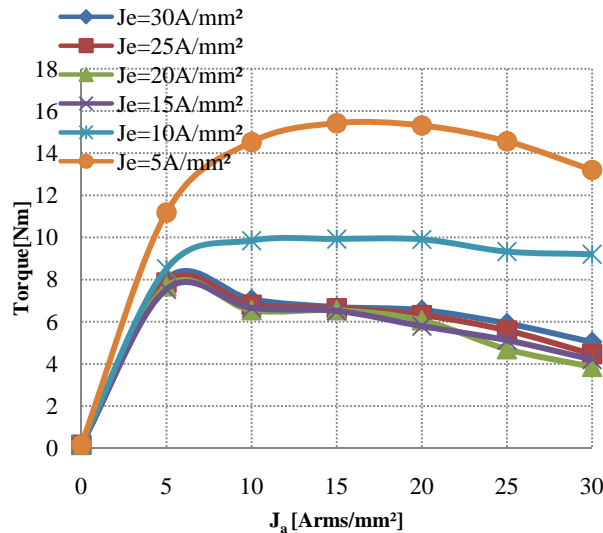


Figure 13. Torque Vs.  $J_a$  at various  $J_e$  for 24S-22P

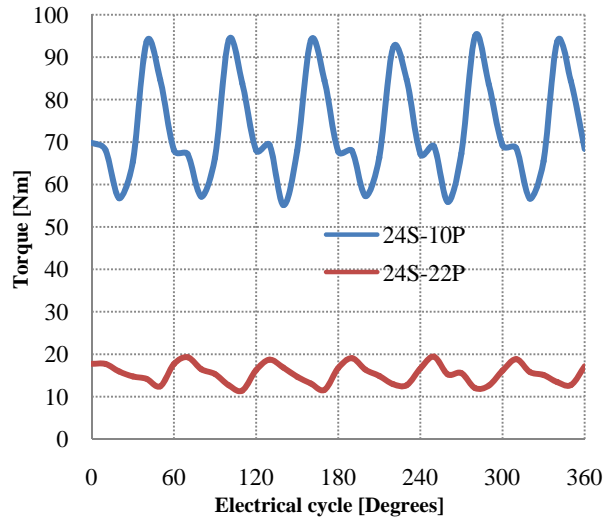


Figure 14. Instantaneous torque characteristics of both WFFSMs

*F. Torque and Power versus Speed Characteristics of 24S-10P WFFSM*

The torque and power versus speed curve of 24S-10P WFFSM is plotted in Figure. 15. At base speed of 965.55 rev/min, the maximum torque of 72.36Nm is obtained for 24S-10P WFFSM. From the figure, it is clear that torque starts to decrease if the machine is operated beyond the base speed. Moreover, 24S-10P WFFSM has high speed at light load condition and the speed reduces by increasing the load. Various speed control methods discussed in [18] can be used in future to operate this motor at variable load conditions and can be adopted to smooth the torque speed characteristic curve. From figure 15, it is obvious that at maximum torque, the power accomplished by 24S-10P WFFSM is 7.31 kW, at the speed of about 965.55 rev/min and reduced at high speed to 5.52kW due to increase in iron loss.

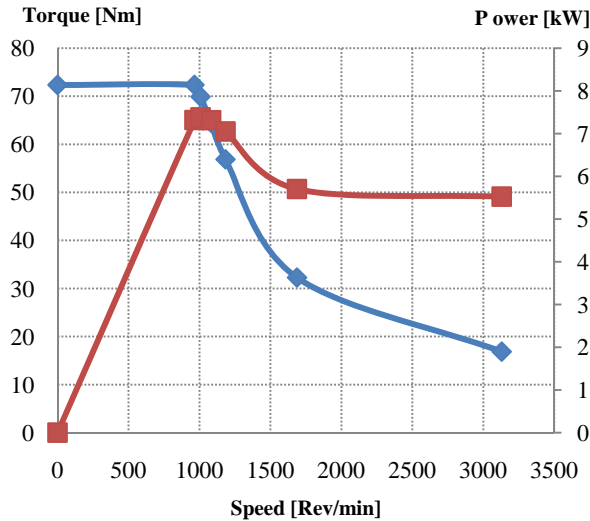


Figure 15. Torque and Power vs. Speed characteristics for 24S-10P

**5. Conclusion**

Five topologies having different pole numbers for three phase wound field flux switching machine have been presented. In comparison with permanent magnet AC machines, it has low

cost due to no permanent magnet and the field flux can be easily controlled. The proposed machine has robust rotor construction and non-overlap windings and thus, it can be defined as simple configuration, low cost and high efficiency machine. Due to replacement of segmental rotor by salient rotor, the mechanical strength of the WFFSM is improved and becomes more suitable for high speed applications. Based on 2D FEA, WFFSMs with 24S-10P and 24S-22P configuration has achieved better performances and can be further improved in future in terms of cogging torque, flux linkage and average torque by design refinement and optimization. With all the analytical investigations, the proposed WFFSMs will definitely give the best result when tested with a prototype model as compared with the previous work did by many researchers.

## 6. Acknowledgements

This work was supported by GIPS Vote No U006 under Research, Innovation, Commercialization and Consultancy management (ORICC), University Tun Hussein Onn Malaysia (UTHM), Batu Pahat, Johor, Malaysia

## 7. References

- [1]. Laws AE. An electromechanical transducer with permanent magnet polarization, Technical Note No.G.W.202, Royal Aircraft Establishment, Farnborough, UK, 1952
- [2]. Rauch SE, Johnson LJ. "Design principles of flux-switching alternators", *AIEE Trans.*, vol.74, no.3, p.1261-1268, Jan 1955.
- [3]. Sulaiman E, Kosaka, T, Matsui N. "High power density design of 6slot-8pole hybrid excitation flux switching machine for hybrid electric vehicles", *IEEE Trans. on Magn.*, vol.47, no.10 pp. 4453-4456, Oct. 2011.
- [4]. Sulaiman E, Kosaka T, Matsui N. "Design optimization and performance of a novel 6-slot 5-pole PMFSM with hybrid excitation for hybrid electric vehicle", *IEEJ Trans. Ind. Appl.*, vol.132, no.2, sec.D, pp.211-218, 2012.
- [5]. E. Sulaiman, M. Z. Ahmad, T. Kosaka, and N. Matsui, "Design Optimization Studies on High Torque and High Power Density Hybrid Excitation Flux Switching Motor for HEV", *Procedia Engineering*, Vol. 53, pp. 312-322, Mar 2013.
- [6]. E. Sulaiman, M. F. M. Teridi, Z. A. Husin, M. Z. Ahmad, and T. Kosaka, "Performance comparison of 24S-10P and 24S-14P field excitation flux switching machine with single DC-coil polarity" *IEEE Int. Power Engineering and Optimization Conference*, pp.46-51, June 2013.
- [7]. J. H. Walker, "The theory of the inductor alternator," *J. IEE*, vol.89, no.9, pp.227-241, June 1942.
- [8]. T. J. E. Miller, "Switched Reluctance Machines and Their Control", Hillsboro, OH: Magna Physics, 1993.
- [9]. B.C. Mecrow, E.A. El-Kharashi, J.W. Finch, and A. G. Jack, "Segmental rotor switched reluctance motors with single-tooth windings", *IEE Proc. on Power Applications*, vol. 150, no. 5, pp. 591-599, 2003.
- [10]. Erwan Bin Sulaiman, Takashi Kosaka, Nobuyuki Matsui "Design Study and Experimental Analysis of Wound Field Flux Switching Motor for HEV Applications" *XXth International Conference on Electrical Machines (ICEM)*, pp.1269 - 1275, Sep 2012.
- [11]. A. Zulu, B.C. Mecrow, M. Armstrong "Topologies for three-phase Wound field Segmented-Rotor flux switching Machines" *5th IET International Conference on Power Electronics, Machines and Drives (PEMD)*, pp.1-6, 2010.
- [12]. Ackim Zulu, Barrie C. Mecrow, Matthew Armstrong "A Wound-Field Three-Phase Flux-Switching Synchronous Motor With All Excitation Sources on the Stator" *IEEE Transactions on Industry Applications*, Vol. 46, No. 6, pp.2363-2371, November/December 2010.
- [13]. H. Pollock, C. Pollock, R. T. Walter, B. V. Gorti, "Low cost, high power density, flux

